Correction of saturated scintillation in RINGSS

Authors:*A. Tokovinin*
Version: 1
Date: 2020-09-10
File: prj/smass/doc/saturcorr.tex

1 Introduction

The theory of all scintillation sensors (MASS, FASS, RINGSS) is based on the small-signal (weak scintillation) approximation which is not quite fulfilled in the real conditions. Spatial spectrum of strong (semi-saturated) scintillation differs from the theoretical (weak-scintillation) spectrum by containing more high-frequency power and less low-frequency power. As a result, the angular power spectrum (APS) $S(m)$ increases at large m, imitating a low-altitude turbulence, and the seeing is over-estimated (over-shoots). This effect was studied in the case of MASS and its partial correction based on numerical simulations was developed (Tokovinin & Kornilov, 2007). The idea is to transform the scintillation variances to their values that would be obtained without saturation, using only the measured signals, and then to apply the standard linear profile restoration algorithm. This strategy was explored in the the pupil-plane case (solid-state MASS or FASS) and it also works. Here it is studied for the ring-image sensor, again using simulations.

2 Effect of strong scintillation
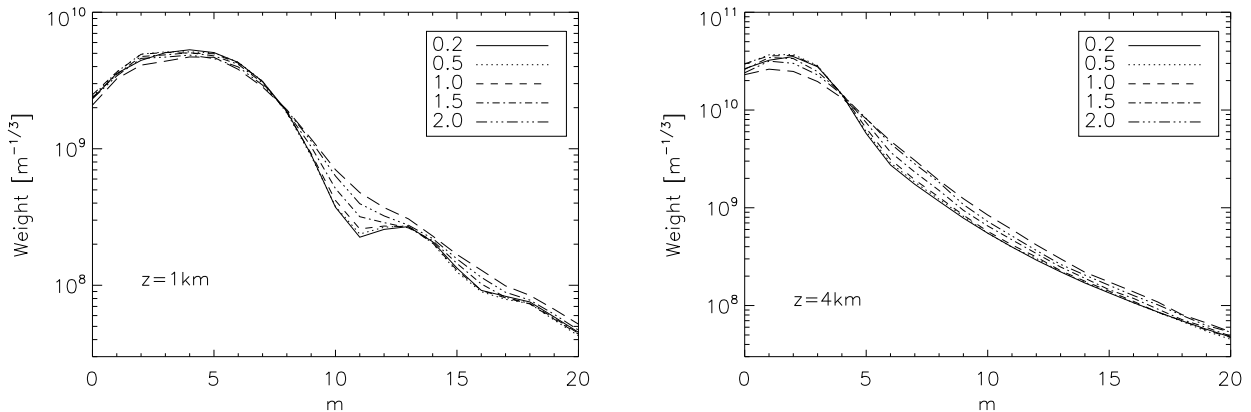
Figure 1: Comparison of analytic WFs (solid line) with WFs from numerical simulation with seeing from $0.2''$ to $2''$ for a single layer at $1\,\mathrm{km}$ (left) and at $4\,\mathrm{km}$ (right).

Figure 1 compares theoretical (weak-scintillation) weighting functions (WFs) with results of simulations for monochromatic light (code `wtbias.pro`) to illustrate the impact of increasingly strong

scintillation. For a turbulent layer at $4\,$km, the classical effect is observed, namely decrease of power at low frequencies (small m) and its increase at intermediate frequencies, $m > 5$. The cross-over occurs at $m = 4$. Note that at $m \sim 20$ the impact of saturation becomes smaller.

For a layer at $1\,$km the overall scintillation is smaller, and the effect of saturation is also moderate below the cross-over at $m = 8$. However, the WF minimum at $m = 11$ is progressively filled. If the effect of saturation is expressed at a ratio of simulated and theoretical WFs (WF bias), there is a strong "spike" around $m = 11$, reaching a factor of two. However, the WFs at those frequencies are already an order of magnitude smaller compared to their maximum. Therefore, the effect of this bias on the restored turbulence profiles (TPs) is negligibly small. Moreover, in polychromatic light this minimum is less deep and, correspondingly, its filling should be less pronounced.

Summarizing, there are two distinct effects of saturation: (i) progressive transfer of power to intermediate frequencies at large z and (ii) partial filling of WF minima at small z. The second effect is specific to RINGSS and is not present when the scintillation is measured at the pupil; it is presumably caused by the interplay between phase and amplitude distortions. This second effect, however, can be neglected in practice, as confirmed below by simulation.

3   Simulations

When the scintillation is measured at the pupil plane, polychromatic light can be simulated by propagation of several wavelengths and averaging the resulting intensity patterns. It is more complex in the case of RINGSS because at each wavelength the image formation must be treated separately. Therefore, this study is based on monchromatic simulations. The effect of spectral bandwidth consists mostly in damping the signal at high frequencies at substantial propagation distances.

The simulation code `bigsimul.pro` randomly selects a seeing value in the range from $0.2''$ to $2''$ and generates two turbulent layers with a 0.8:0.2 ratio of turbulence power (i.e. turbulence integrals J_i) using `simatm.pro`. The distances z_i are chosen randomly from a log-spaced grid with a step of $\sqrt{2}$, ranging from $0.5\,$km to $16\,$km. Monochromatic waves are propagated through these layers and the simulated image cubes are generated using `ringsim.pro` with the instrument parameters specified in `sim1.par` (telescope diameter $0.13\,$m, central obscuration 0.5, pixel size $1.55''$, wavelength $0.6\,\mu$m, effective conjugation to $-400\,$m). The strength of the scintillation is characterized by the intensity variance s_0^2, usually called Rytov number (or variance):

$$s_0^2 = 19.12\lambda^{-7/6} \sum J_i z_i^{5/6}. \tag{1}$$

Only cases with s_0^2 from 0.02 to 1 are used to avoid too weak or too strong scintillation. A total of 500 realizations are computed. Theoretical (i.e. small-signal) APS S_m^{theo} computed using the WFs is compared to the measured APS S_m. The total power $S_{\text{tot}} = \sum_m S_m$ is a measure of the scintillation strength. As shown in Fig. 2, the total power is a good proxy for the unknown Rytov variance when the scintillation is strong.

The main set of simulations produced by `bigsimul.pro` contains 500 cases. The results (measured and theoretical indices, altitudes, etc.) are saved and used for development of the correction algorithm. Other, smaller sets of simulations (e.g. with equal layers) were also generated. For one set of 100 cases the data cubes are saved and processed by the standard pipeline to produce the control sample.

2
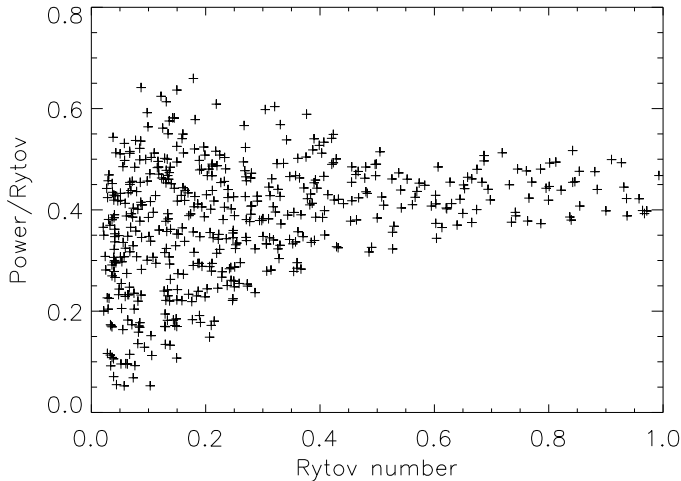
Figure 2: Ratio of the total measured power S_{tot} to the Rytov variance s_0^2 in the simulations.

4 Correction algorithm

The saturation correction is based on linear combinations of the measured APS S_m with coefficients adjusted to reach the best match between theoretical and corrected (quasi-linear) power, similarly to the method used in MASS. The set of these coefficients, derived for each m, represents the correction matrix $Z_{m,k}$, or Z-matrix (Tokovinin & Kornilov, 2007). The analysis indicates that only a few terms involving the lowest-m signals are useful, because the correction quality does not improve further with increasing number of coefficients. The ratio of the measured APS S_m to the unknown (small-signal) APS S_m^{theo} is modeled as

$$S_m/S_m^{\mathrm{theo}} \approx 1 + \sum_{k=1}^{5} Z_{m,k} S_k, \tag{2}$$

where the sum includes a restricted number of terms from $k = 1$ (the $k = 0$ term is not used) to 5. The correction from measured to quasi-linear signal is the inverse of the right-hand part; it approaches one as the scintillation tends to zero.

This model was studied in the case of pupil-plane turbulence sensor and shown to work; typically the first 5 terms are sufficient. Alternative flavors of correction algorithms were probed, but they performed less well. For RINGSS, I probed a simplified version with a single parameter Z_m multiplied by S_{tot}, replacing the linear combination in eq. 2. This linear correction works, but less well than the matrix correction with 5 terms adopted finally. Alternatively, I considered a matrix correction involving 3 terms S_1, $S_2 + S_3$, and , $S_3 + S_4 + S_5$. It gives good results, but computationally is not simpler than the full matrix correction with 5 terms. Including the S_0 term does not improve the correction.

The correction is determined and evaluated by the procedure `zmatrix2` in `bigtest.pro`. Equation (2) is transformed to

$$\sum_k S_k Z_{m,k} = Y_m, \quad Y_m = S_m/S_m^{\mathrm{theo}} - 1. \tag{3}$$

Here Y_m is the vector of length 500 (total number of simulations), S_k is a subset of APS from 1 to 5

3

for each simulation, i.e. the matrix $\mathbf{S}$ of the size 500×5, and $Z_{m,k}$ is the m-th line of the Z-matrix. For each m, equation (3) is solved to find $Z_{m,k}$ by the standard least-squares method. Let $A = (\mathbf{S})^T\mathbf{S}$ be the system matrix. Then the solution is

$$Z_m = A^{-1}[\mathbf{S}^T Y_m]. \tag{4}$$

Two subtleties are involved. First, only simulation results with Rytov variance from 0.05 to 0.7 are used and the cases with the lowest layer at or below 1 km are excluded. This "training set" of 149 cases (out of 500) is used to find Z, and the resulting rms difference between theoretical and corrected signals is computed for the training set and for the full set. Second, the inversion of A is done by SVD with rejection of singular values below 10^{-3} of the largest singular value to avoid noise amplification. Typically, 3 singular values are rejected.
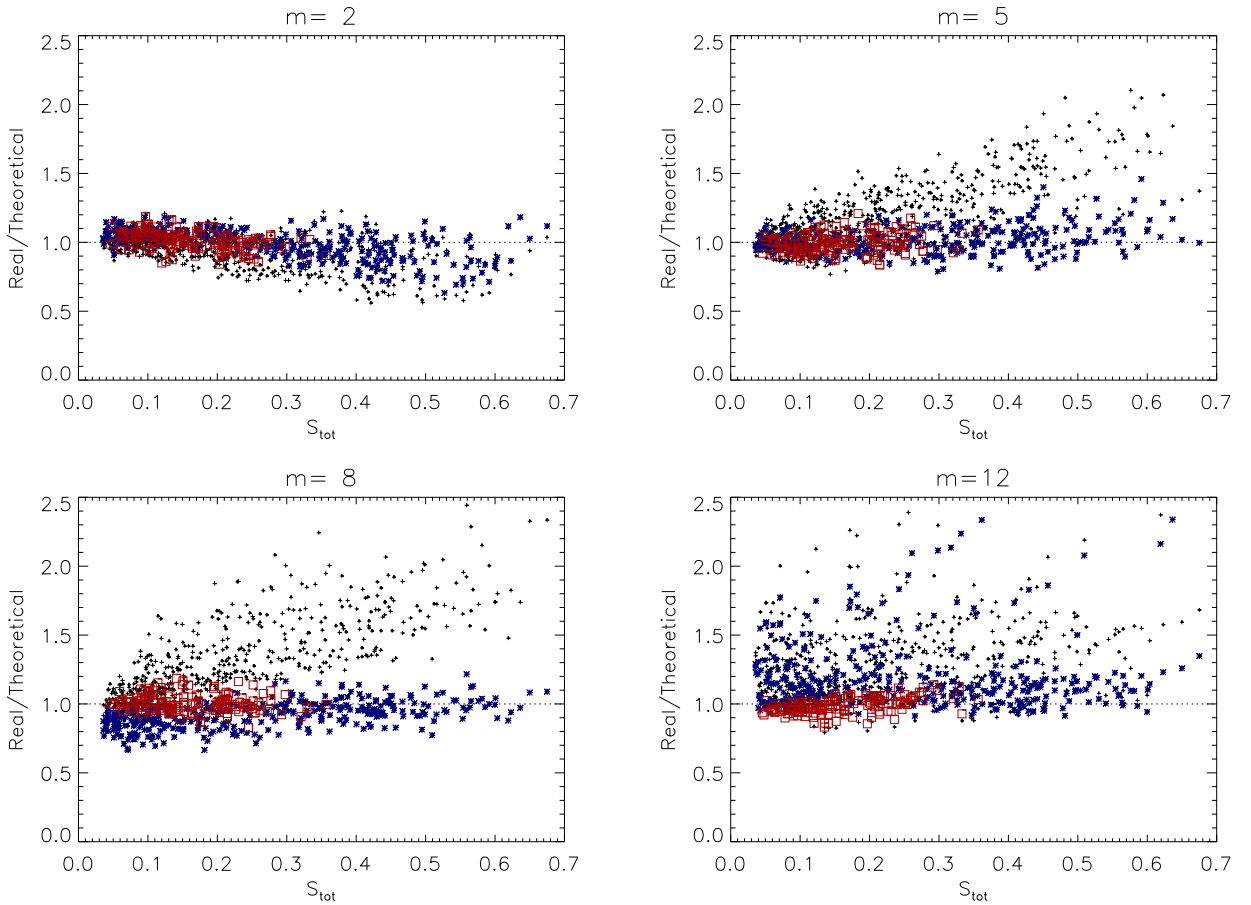
Figure 3: Ratio of uncorrected to theoretical power S_m/S_m^{theo} (crosses), ratio of corrected power for the training set (red squares) and for the remaining cases (blue asterisks) plotted against S_{tot} for terms $m = 2$, $m = 5$ (top) and $m = 8$, $m = 12$ (bottom).

The matrix correction was studied for all m from 1 to 20 that are used in the profile restoration. Figure 3 gives representative plots. The quality of the correction is estimated by the rms of the

Table 1: Correction quality and Z-matrix

m	Uncorr. rms	Training set rms	All rms	Z_1	Z_2	Z_3	Z_4	Z_5
1	0.13	0.08	0.10	0.2	3.8	-0.2	-3.0	-3.1
2	0.13	0.07	0.09	0.1	-1.1	-1.1	-0.6	-0.3
3	0.18	0.06	0.08	1.9	-0.5	-2.9	-3.3	-2.5
4	0.23	0.05	0.07	4.2	1.6	-4.4	-6.4	-5.3
5	0.26	0.07	0.09	1.3	9.6	-2.9	-10.8	-10.5
8	0.29	0.06	0.10	1.6	-3.1	6.0	10.7	9.4
9	0.30	0.09	0.11	4.0	-9.4	6.1	16.0	14.9
10	0.28	0.07	0.13	5.2	-12.2	5.5	17.4	16.7
12	0.31	0.06	0.23	-0.5	-2.9	4.8	8.6	7.5
15	0.20	0.05	0.14	0.9	-6.0	3.4	9.2	8.6

ratio $S_m^{\mathrm{corr}}/S_m^{\mathrm{theo}}$ computed separately for the training set and for the full set. Sample of these rms values and the rms differences without correction is given in Table 1 together with the Z-matrix lines. Overall, the correction works quite well and the rms for the training set are between 0.05 and 0.09. The largest impact of saturation and, correspondingly, the largest correction is found for $m = 9$; the $m = 1$ and $m = 2$ terms have the smallest correction.

Looking at Fig. 3, one notes that for $m = 5$ and $m = 8$ the correction works very well not only for the training set, but also for the full set; the rms for the full set is within 0.1. However, for $m = 12$ some blue asterisks are well above one, while the rms for the full set, 0.23, is almost as large as 0.31 without correction. These deviant points correspond to the cases with layers below 1 km, where the minima of the WFs are filled (see Fig. 1, left). This phenomenon is not corrected by the current algorithm and this is the reason why the low-z cases are removed from the training set. The mixture of two different phenomena related to strong scintillation complicated development of the correction algorithm for RINGSS.

5 Testing

A quick simulation run of 100 1-second data cubes (1000 frames each) was processed by the pipeline. In the profile restoration code `profrest4.pro`, the correction for finite exposure was disabled (the simulations did not include the blur), and the Z-matrix correction was either enabled or disabled. Figure 4 compares the total estimated seeing with the simulated one. In the left-hand panel we note the "overshoots" caused by partially saturated scintillation. Energy spilled to higher frequency is interpreted as coming from lower but stronger layers, and the seeing is over-estimated. When the Z-matrix correction is switched on, the over-shoots disappear. Note that the seeing is estimated reasonably well from only 1000 simulated frames.

The seeing deduced from the differential sector motion is under-estimated (under-shoots). This is caused by two distinct effects illustrated in Fig. 5. First, propagation reduces the phase fluctuations and, correspondingly, the differential sector motion. Second, the sector motion is further reduced under strong scintillation, as shown in the rigt-hand panel. The empirical correction factor $0.87(1 - 0.78 S_{\mathrm{tot}})$ could be applied to reduce both biases, but it is better to treat them separately. Similar effects are
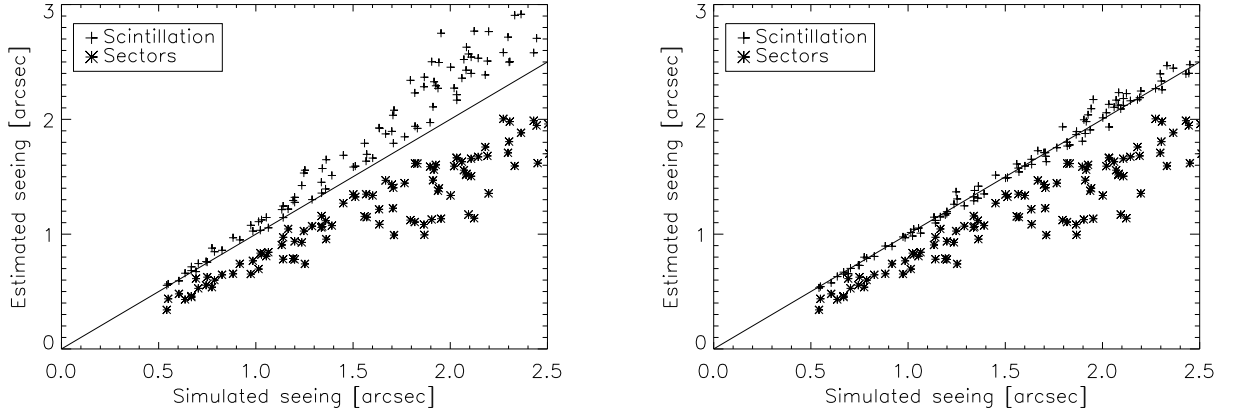
Figure 4: Seeing deduced from the turbulence profiles restored from APS (crosses) and estimated from the differential sector motion (asterisks) is plotted against simulated seeing, with the straight line corresponding to equality. Left: without saturation correction, right: with correction.
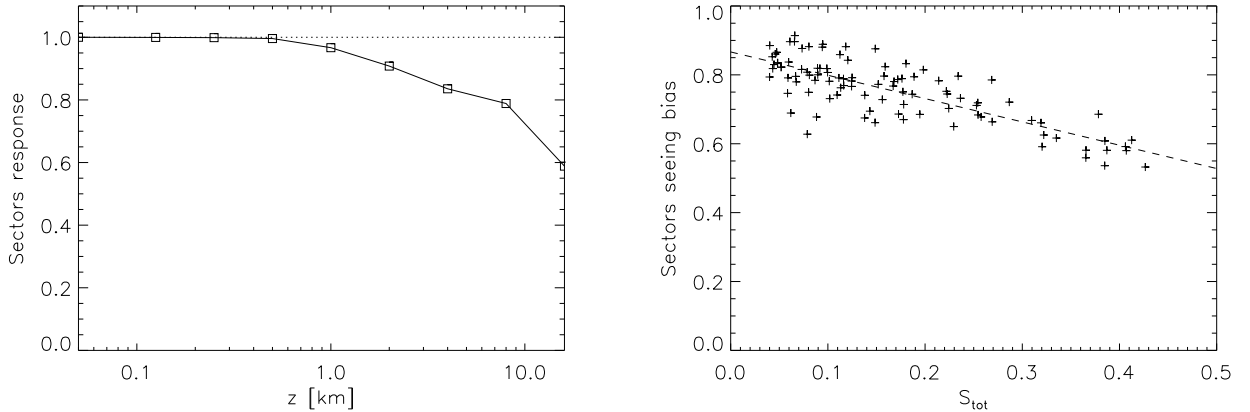
Figure 5: Explanation of bias in the seeing estimated from the differential sector motion. Left: relative response in the weak-scintillation rgime showing reduction of the variance with increasing z. Right: ratio of the estimated and true seeing as function of the scintillaion strength S_{tot}. The dashed line is a linear fit $0.87(1 - 0.78 S_{\mathrm{tot}})$.

encountered in DIMM (Tokovinin & Kornilov, 2007). Typical DIMMs have larger apertures compared to RINGSS, reducing the impact of diffraction. However, even a standard DIMM needs corrections for propagation and partial saturation that are not implemented in the existing site monitors.

Figure 6 gives additional insight into over-shoots by plotting the simulated (input) turbulence profile and the retrieved profile. The simulated seeing was $2.12''$, with 0.8 fraction at $4\,\mathrm{km}$ and 0.2 at $16\,\mathrm{km}$, resulting in a strong scintillation of $S_{\mathrm{tot}} = 0.55$. The estimated seeing is $2.22''$ and $2.77''$ with and without correction, respectively. Without correction, the restored profile is shifted to a closer

6
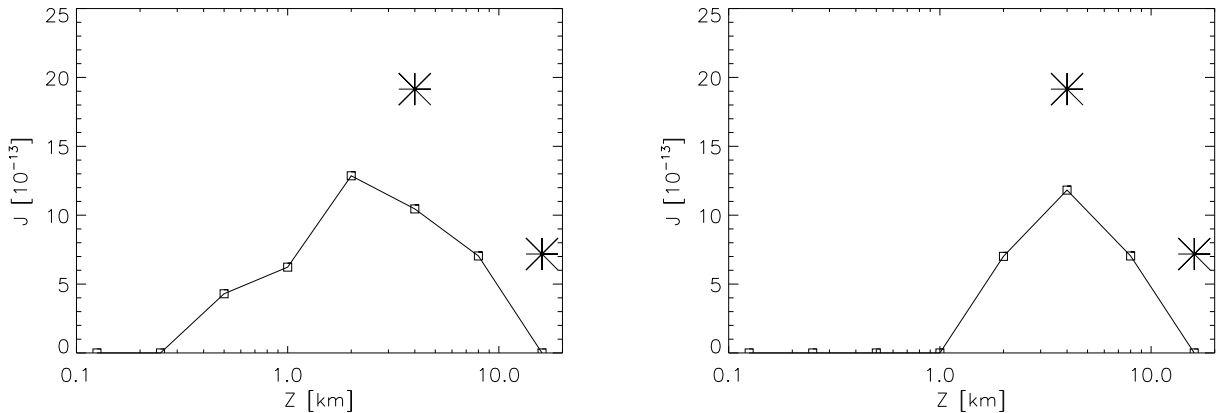
Figure 6: Simulated turbulence profile (asterisks) and the restored profile (line) for one simulation with $S_{\mathrm{tot}} = 0.55$. Left: without saturation correction, right: corrected.

distance. Correction improves the result, but it is still far from perfect. Interestingly, the mean rms residuals between measured and modeled APS are substantially smaller without correction. A similar situation was found in MASS: the restoration algorithm happily models the biased signal by placing turbulence at a closer range. This means that the rms residuals to APS fits are not suitable as a metric of the accuracy of result.

6   Conclusions

The proposed algorithm gives an empirical solution to turbulence profile restoration for moderately saturated scintillation. This regime is frequently encountered in practice, and the correction seems to be necessary; otherwise the seeing and free-atmosphere seeing become over-estimated. However, these over-shoots remain modest (mostly within 10%) and can be considered as tolerable, especially at good sites. After all, turbulence parameters are always measured with a varying degree of approximation.

The phenomenon of saturated scintillation is generic, but the correction matrix depends on the instrument parameters. A tool to estimate the Z-matrix from simulations for an arbitrary instrument will be developed by adaptation of existing code. The general character of the correction (decrease at small m and overshoots at large m) is valid for any instrument.

References

Tokovinin A., Kornilov V., 2007, MNRAS, 381, 1179